



# Microcantilever-based label-free characterization of temperature-dependent biomolecular affinity binding

Bin Wang<sup>a</sup>, Fengliang Huang<sup>a,b</sup>, ThaiHuu Nguyen<sup>a</sup>, Yong Xu<sup>c</sup>, Qiao Lin<sup>a,\*</sup>

<sup>a</sup> Department of Mechanical Engineering, Columbia University, New York, USA

<sup>b</sup> School of Electrical & Automation Engineering, Nanjing Normal University, Nanjing, China

<sup>c</sup> Department of Electrical and Computer Engineering, Wayne State University, Detroit, USA

## ARTICLE INFO

### Article history:

Received 3 November 2011

Received in revised form 10 February 2012

Accepted 18 February 2012

Available online 9 October 2012

### Keywords:

Aptamer

Affinity binding

Microcantilever

Label-free detection

Temperature dependence

## ABSTRACT

This paper presents label-free characterization of temperature-dependent biomolecular affinity binding on solid surfaces using a microcantilever-based device. The device consists of a Parylene cantilever one side of which is coated with a gold film and functionalized with molecules as an affinity receptor to a target analyte. The cantilever is located in a poly(dimethylsiloxane) (PDMS) microfluidic chamber that is integrated with a transparent indium tin oxide (ITO) resistive temperature sensor on the underlying substrate. The ITO sensor allows for real-time measurements of the chamber temperature, as well as unobstructed optical access for reflection-based optical detection of the cantilever deflection. To test the temperature-dependent binding between the target and receptor, the temperature of the chamber is maintained at a constant setpoint, while a solution of unlabeled analyte molecules is continuously infused through the chamber. The measured cantilever deflection is used to determine the target–receptor binding characteristics. We demonstrate label-free characterization of temperature-dependent binding kinetics of the platelet-derived growth factor (PDGF) protein with an aptamer receptor. Affinity binding properties including the association and dissociation rate constants as well as equilibrium dissociation constant are obtained, and shown to exhibit significant dependencies on temperature.

© 2012 Elsevier B.V. All rights reserved.

## 1. Introduction

Biomolecular affinity binding is of fundamental importance for a wide variety of biological processes in that conformational and chemical complementarity between the binding molecules strongly influences cellular signal transduction and expression [1]. Modern drug development and therapeutics have thus increasingly relied on biomolecular binding studies [2]; current experimental and computational screening of compounds for therapeutic drugs is often based on interrogation of ligand–receptor binding affinity [3]. Since the binding affinity commonly involves thermodynamic activity and is determined by the Gibbs energy during the biomolecular interaction [3], consideration of temperature effects is crucial in therapeutic ligand design. In addition, as *in vivo* relevant therapeutic assays have become increasingly important, insight into the temperature-dependent nature of biomolecular affinity binding [4,5] can be critical for understanding the mechanisms governing these interactions, such as the efficacy of drug molecules under thermally active stimulation [6]. Moreover, knowledge about the temperature dependence of ligand–receptor systems can assist in

identifying therapeutic targets by exploring receptor dysfunction associated with metastatic cell proliferation, or receptor recovery leading to tissue repair [7]. One clinically significant example is the development of inhibitory ligands for platelet-derived growth factor (PDGF), a protein regarded as an ubiquitous mitogen and chemotactic factor [8] in angiogenesis. If the inhibitory ligands to PDGF are used *in vivo*, it is crucial to understand the temperature-dependence underlying PDGF–ligand interaction. Therefore, there is a strong need for a technique that can reliably characterize the effects of temperature on biomolecular affinity binding.

Affinity binding can occur with target and receptor molecules in solution, or with either molecule immobilized to solid surfaces. Solution-based affinity binding is commonly characterized using methods such as UV-absorption [8], differential and titration calorimetry [9], matrix-assisted laser desorption/ionization mass spectrometry (MALDI-MS) [10] and electrophoretic separation [11]. Surface-based affinity binding, which is widely used in affinity biosensors [12], can be investigated with methods such as protein arrays [13], immunoassays [14], and thermal-shift assays [15], which use fluorescent or radioactive labeling groups to signal binding events. Such labeling of target or receptor molecules is in general time-consuming and labor intensive, and is not capable of distinguishing signals from analytes in inactive and active forms [16]. More importantly, when used for temperature-dependent

\* Corresponding author. Tel.: +1 212 854 1906.

E-mail address: [qlin@columbia.edu](mailto:qlin@columbia.edu) (Q. Lin).



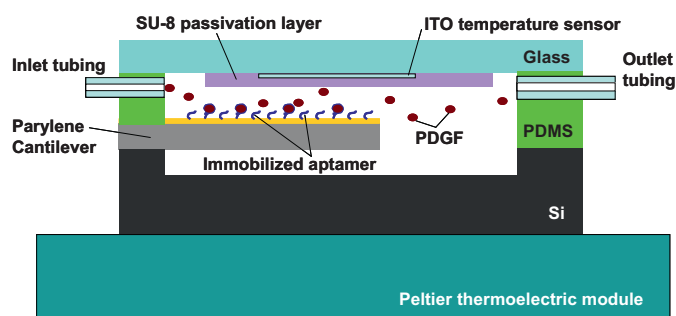


**Fig. 3.** Design schematic of the cantilever-based microfluidic device for characterization of temperature-dependent aptamer–PDGF binding.

during experiments. Temperature is controlled in closed loop by adjusting the voltage applied to the Peltier module (which allows both heating and cooling by thermoelectric effects [32]) according to the feedback from the in-situ ITO temperature sensor. Transparent ITO patterned glass is chosen for unobstructed optical detection of microcantilever deflection. Parylene is employed as a device material to exploit benefits such as higher potential detection sensitivity due to its low Young's modulus and excellent chemical inertness.

The fabrication of the microcantilever chip began on an oxide-precoated silicon wafer. Multiple cantilevers were included in the chamber for redundancy. First, anchor cavities surrounding the cantilevers were defined and etched by KOH to a depth of approximately 20  $\mu\text{m}$  (Fig. 4(a)). Then the pits underneath the cantilevers were defined, followed by uniformly coating a 6  $\mu\text{m}$  thick Parylene film via chemical vapor deposition (CVD) (Fig. 4(b)). Cantilevers were then patterned by oxygen–plasma reactive ionic etching (RIE), and coated with a Cr/Au (5/45 nm) thin film via thermally evaporation and wet etching (Fig. 4(c)). Subsequently, the pits defined above were completed by  $\text{XeF}_2$  gas-phase etching to fully release the cantilevers (Fig. 4(d)). In parallel, the ITO temperature sensor was patterned on an ITO-coated glass slide (Delta Technologies, CB-50IN) by wet etching using 25% HCl (Fig. 4(e)) and passivated by a 1.5  $\mu\text{m}$  thick SU-8 photoresist layer (Fig. 4(f)). Also, a 250  $\mu\text{m}$  thick PDMS spacer layer defining the microfluidic chamber was

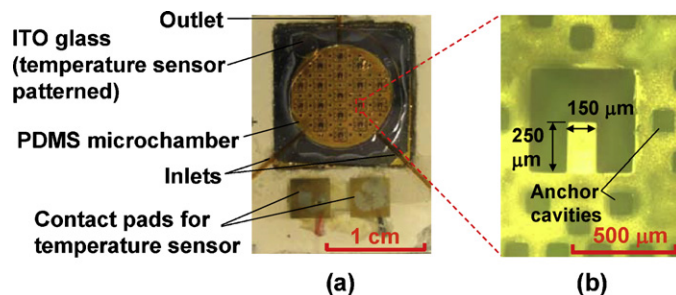


**Fig. 5.** Fabricated microcantilever device. (a) Image of a packaged device. (b) Micrograph of a representative single cantilever.

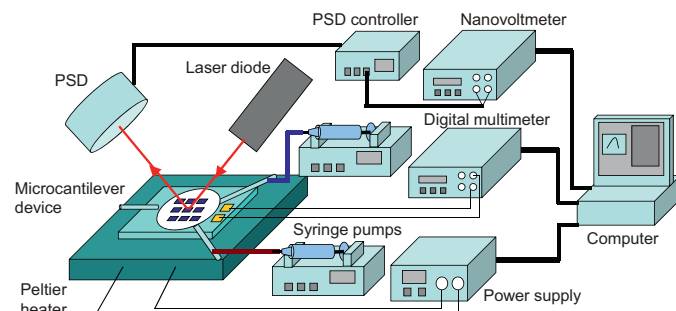


**Fig. 6.** Experimental setup for the temperature control, optical detection and signal acquisition in the cantilever-based microfluidic device.

fabricated using a replica molding technique [33] (Fig. 4(g)). Finally, the microcantilever chip, the PDMS spacer layer, and the ITO glass slide were bonded together in sequence with the interfaces treated with oxygen plasma and reinforced by gluing (Fig. 4(h)). The inlet and outlet solution lines were coupled to the device by capillary tubings inserted into the PDMS spacer layer. The resulting chip package was attached to a Peltier module (Melcor) using a thermally conductive glue (Omega Engineering). Fig. 5(a) shows a packaged device with 17 microcantilevers in a circular chamber and Fig. 5(b) the micrograph of a representative single cantilever.

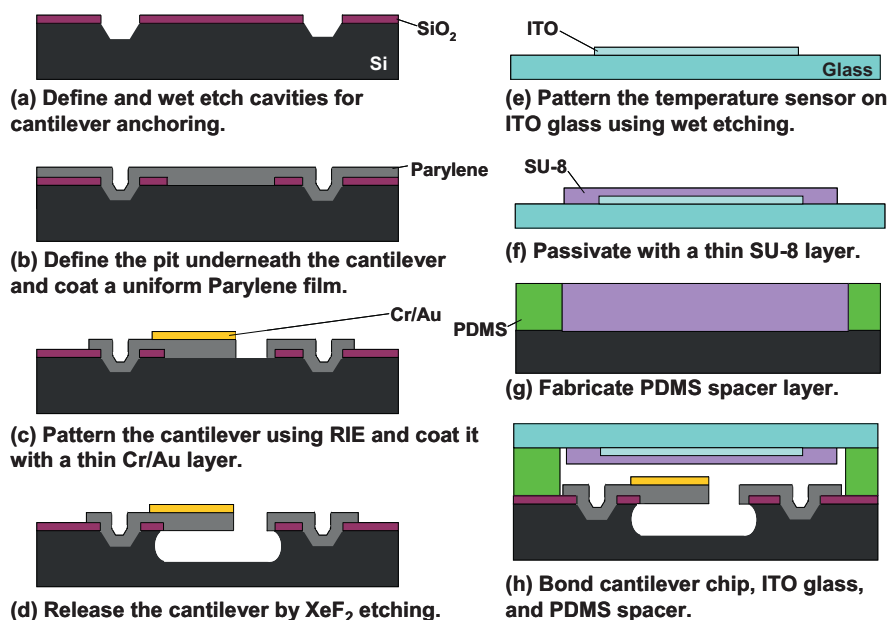


**Fig. 4.** Fabrication process of the microcantilever device.

As shown in Fig. 6, the experimental setup mainly consisted of electrical instruments for temperature control, and an optical lever for optical detection. The temperature inside the reaction chamber of the chip was maintained at a desired setpoint using the Peltier thermoelectric module driven by a DC power supply (Agilent E3631) and the ITO temperature sensor measured by a digital multimeter (Agilent 34410A), regulated under closed-loop proportional-integral-derivative (PID) control algorithm. During experiments, the two inlets were connected to two parallel solution lines driven by syringe pumps (New Era Pump Systems NE-1000) which allowed convenient switch between two different injected solutions. For optical detection, a home-built optical lever system was used, in which a laser beam from a diode laser generator was directed to the gold surface of a cantilever and reflected to a photosensitive detector (PSD, Coherent). The signal was amplified by a PSD amplifier (Photonics OT-301) and then measured by a nanovoltmeter (Agilent 34420A). The on-chip temperature control and optical signal acquisition were computer-automated and monitored by a LabVIEW-based program.

### 2.3. Materials and experimental procedure

An isoform of PDGF, PDGF-BB (Sigma Aldrich), was chosen as a model analyte in our experiments. PDGF-BB was prepared in PBSM buffer (10.1 mM Na<sub>2</sub>HPO<sub>4</sub>, 1.8 mM KH<sub>2</sub>PO<sub>4</sub>, 137 mM NaCl, 2.7 mM KCl, and 1 mM MgCl<sub>2</sub>, pH 7.4). The PDGF-specific aptamer was obtained from IDT DNA and prepared in sterile water (Fisher Scientific). All solutions were degassed prior to introduction into the microfluidic chambers to avoid inducing air bubbles. Meanwhile, the microcantilever device was pre-cleaned with acetone, ethanol, and sterile water sequentially. To immobilize aptamer molecules on the cantilever surface, 3  $\mu$ M aptamer solution was allowed to perfuse through the reaction chamber overnight at a constant flow rate of 0.5  $\mu$ L/min at 4 °C. During the aptamer–PDGF association and dissociation experiments, PBSM buffer and 5 nM PDGF solutions respectively perfused through the reaction chamber via the device's two microfluidic inlets as follows. The chamber was initially flushed with PBSM buffer and then infused with PDGF solution, initiating the association between PDGF and the aptamer as detected via the cantilever deflection. After the association reached equilibrium, the infusion was switched back to PBSM buffer to enable the dissociation process. Throughout the experiments, the flow rate of both PBSM buffer and PDGF solution was maintained at 10  $\mu$ L/min, which was chosen to allow an acceptable mass transport rate at which PDGF molecules were accessed by the aptamer-functionalized surface [34], while limiting the flow-induced shear force on the molecules that could affect the binding activity [35]. After the measurement, the system was regenerated by removing any PDGF molecules that remained on the surface by 4 M urea and 15 mM EDTA and then rinsing with PBSM buffer. The baseline in response signal, i.e., the PSD output of the optical detection system with no occurrence of the aptamer–PDGF affinity binding, was measured with PBSM buffer alone flowing through the microchamber.

### 2.4. Monovalent binding kinetic model

We consider a monovalent model for the equilibrium affinity binding between the immobilized receptor (of concentration  $[R]$ ) and the target analyte (of concentration  $[A]$ ) to form a complex (of concentration  $[RA]$ ) [36]:



where  $k_{\text{on}}$  and  $k_{\text{off}}$  are the association and dissociation rate constants, respectively. The net rate of complex formation varies with time according to the following differential equation:

$$\frac{dy}{dt} = k_{\text{on}} [A](y_{\text{max}} - y) - k_{\text{off}} y \quad (2)$$

where  $y$  and  $y_{\text{max}}$  respectively represent the observed response signals respectively corresponding to the complex concentration  $[RA]$  and saturation complex concentration  $[RA]_{\text{max}}$  (i.e., the asymptotic value of  $[RA]$  at infinite time) for a given concentration of injected analyte  $[A]$ .

In flow-through mode as used in the experiments, either the target analyte solution (for association) or pure buffer (for dissociation) is introduced continuously to the cantilever. At a sufficiently large flow rate, the analyte concentration  $[A]$  can be assumed to be a constant  $c$  in the association process, or 0 in the dissociation process [36]. Eq. (2) thus reduces to the following equations, respectively, for the association and dissociation processes:

$$\frac{dy}{dt} = k_{\text{on}} c(y_{\text{max}} - y) - k_{\text{off}} y \quad (3)$$

$$\frac{dy}{dt} = -k_{\text{off}} y \quad (4)$$

Solving Eq. (3) (using initial condition  $y=0$  at  $t=0$ ) yields the time-dependent association response signal:

$$y = y_{\text{max}} \frac{c}{K_d + c} (1 - e^{-(k_{\text{on}}c + k_{\text{off}})t}) \quad (5)$$

where  $K_d = K_{\text{off}}/K_{\text{on}}$  is the equilibrium dissociation constant.

For the dissociation process, solving Eq. (4) yields

$$y = y_0 e^{-k_{\text{off}}t} \quad (6)$$

where  $y_0$  is the initial signal at the beginning of the dissociation process ( $t=0$ ). Using Eqs. (5) and (6), the kinetic and equilibrium binding constants ( $k_{\text{on}}$ ,  $k_{\text{off}}$ , and  $K_d$ ) can be obtained from the time-resolved measurement signal  $y$ .

## 3. Results and discussion

### 3.1. Aptamer–PDGF binding and selectivity to PDGF

We first validated the specificity of PDGF binding in our device with three sets of control experiments. These include (1) introduction of PDGF solution into the reaction chamber with an aptamer-free cantilever surface, followed by PBSM buffer; (2) introduction of only PBSM buffer into the reaction chamber of an aptamer-functionalized cantilever; and (3) introduction of a lysozyme (egg white, Sigma Aldrich) solution to an aptamer-functionalized cantilever, followed by PBSM buffer. Here lysozyme, which has comparable molecular weight (14.3 kDa) to PDGF (25 kDa), was used as a non-binding protein for testing the aptamer specificity.

Fig. 7 shows the signal traces of the control experiments, combining the phases of sample injection and PBSM buffer injection, compared with a representative trace of aptamer–PDGF binding undergoing the same phases. Throughout the experiments, this device showed a noise level of less than  $\pm 2$  mV and repeatability within 10%. In the absence of either aptamer or PDGF, no signal above noise level was detected upon the presence of biomolecules or buffer solution. More importantly, for aptamer–PDGF binding, there existed an exponential increase to a binding equilibrium corresponding to the introduction of PDGF molecules, and a relatively slow shift back to the original equilibrium upon PBSM buffer injection. Thus, the non-specific binding of PDGF to either surface of the cantilever was generally negligible compared with the affinity binding between aptamer and PDGF.



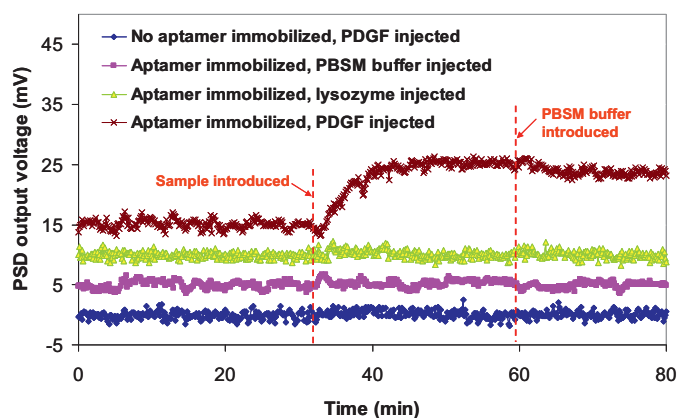


**Fig. 7.** Binding specificity demonstrated by association and dissociation signal traces of control experiments in the absence of either aptamer or PDGF, compared with a representative aptamer–PDGF binding trace (all traces intentionally plotted with an offset of 5 mV for clarity).

### 3.2. Characterization of temperature-dependent aptamer–PDGF binding

Temperature-dependent characterization of the aptamer–PDGF binding was performed by monitoring the association and dissociation processes at temperature varying from 19 to 37 °C. This temperature range is considered suitable for characterization of aptamer–PDGF interactions since aptamer-based therapeutics typically demand a physiologically relevant temperature up to 37 °C. With our experimental setup, the temperature inside the chamber, indicated by the ITO temperature sensor, was consistently controlled within  $\pm 0.3$  °C at setpoints in the range of 19–37 °C. The experimental data were then fitted to the monovalent binding kinetic model given in Eqs. (5) and (6) to obtain the temperature-dependent kinetic properties of the rate constants for association ( $k_{on}$ ) and dissociation ( $k_{off}$ ), and the equilibrium dissociation constant ( $K_d$ ). For each temperature setpoint, we used the GraphPad Prism software [37] to fit the experimental data on the combined dissociation and association processes in a manner that ensures the baseline consistency.

Fig. 8 shows the experimental signal (baseline subtracted) of aptamer–PDGF association and dissociation processes at controlled temperature setpoints of 19, 25, 31, and 37 °C, as well as the fitted curves to the monovalent binding kinetic model. These data showed a clear shift with temperature, and thus considerable temperature dependence within the aptamer–PDGF interaction.

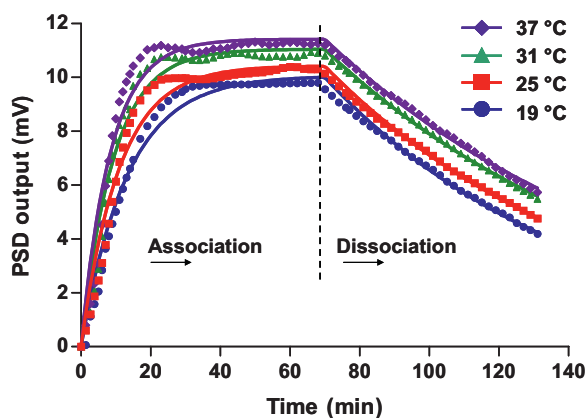


**Fig. 8.** The experimental data of association (left) and dissociation (right) processes at 19, 25, 31, and 37 °C and the fitted curves to the monovalent binding kinetic model.

In particular, as the temperature increased from 19 to 37 °C, the characteristic time for the association process to reach equilibrium decreased from approximately 30–15 min, indicating that the rate of the aptamer–PDGF association process increased with temperature. In addition, the steady-state deflection of the cantilever in equilibrium aptamer–PDGF binding also increased with temperature (Fig. 8). This indicated a more significant surface stress change on the cantilever, which was primarily caused by a larger fraction of immobilized aptamer molecules that are bound to PDGF molecules. These results suggest that temperatures in the physiological range present an optimal condition for the binding of PDGF to aptamer, which is determined by a combination of aptamer tertiary conformation, molecular orientation, and binding energy, as well as the effect of generally increased Brownian motion at higher temperature.

There was a small apparent overshoot in the detected signal before the association process reached equilibrium (Fig. 8). This could be attributed to the variation in the flow rates during the introduction of PBSM buffer and PDGF solution to the microchamber, which most likely were caused by the difference in the syringe pumps and access channels between PBSM buffer and PDGF solution injections. As the association process was triggered by switching the introduction of PBSM buffer to that of PDGF solution, the variation in flow rate induced a difference in the hydrodynamic force on the cantilever and in turn a slight overshoot in cantilever deflection. However, this did not significantly influence the values of binding parameters obtained from the model (Eqs. (5) and (6)) to the experimental data.

In the flow-through experiments, the mass transport of biomolecules occurred by convection and diffusion. To assess this effect on the aptamer–PDGF binding in our device, we first estimated the characteristic time for PDGF molecules accessed by the cantilever surface. The rate of molecular transport to the surface is given by the Onsager coefficient of mass transport [34]:

$$k_m \approx \sqrt[3]{\frac{D^2 u}{h^2 b l}} \quad (7)$$

where  $D$  is the diffusivity of sample biomolecules,  $u$  is the flow rate for sample introduction,  $h$  is the height of the reaction chamber, and  $b$  and  $l$  are the width and length of the cantilever. For the experimental data above,  $h = 250$   $\mu\text{m}$ ,  $b = 150$   $\mu\text{m}$ ,  $l = 250$   $\mu\text{m}$ , and  $D \approx 10^{-10}$   $\text{m}^2/\text{s}$  [38]. Using  $u = 10$   $\mu\text{L}/\text{min}$ ,  $k_m = 5.4 \times 10^{-4}$   $\text{m}/\text{min}$ , and the time scale for the analyte diffusion was estimated to be  $h/k_m = 0.46$  min. Compared with the apparent time scale of aptamer–PDGF association process (approximately 15–30 min), it is reasonable to assume that the aptamer–PDGF binding process was not limited by mass transport at this flow rate [34].

We further determined the kinetic and equilibrium binding properties by fitting the monovalent binding model (Eqs. (5) and (6)) to the experimental data. The temperature dependent kinetic binding rate constants are shown in Fig. 9. As the temperature increased from 19 to 37 °C,  $k_{on}$  increased from  $1.3 \times 10^7$  to  $2.3 \times 10^7$  ( $\text{M min})^{-1}$ , while  $k_{off}$  decreased from 0.015 to 0.01  $\text{min}^{-1}$ . Meanwhile,  $K_d$ , as shown in Fig. 10, decreased from approximately  $12 \times 10^{-10}$  M to  $5 \times 10^{-10}$  M as the temperature changed from 19 to 37 °C. This indicates stronger aptamer–PDGF binding, i.e., a more favorable conformational change of the aptamer molecules for the affinity interaction as the temperature approached the physiological values, at which the aptamer was synthetically isolated [8]. Moreover, the decrease of  $K_d$  with temperature implies that the aptamer–PDGF system becomes more thermodynamically stable as the temperature increases, which typically involves negative Gibbs free energy [3]. These results are consistent with published data using conventional methods (e.g., UV-absorption [8]). The  $K_d$  values we obtained are higher than those obtained with the aptamer

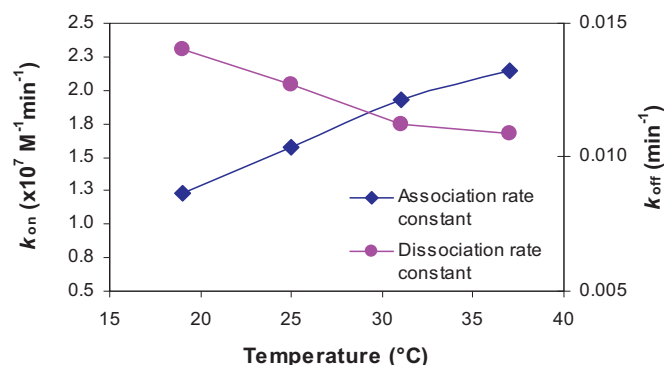


Fig. 9. Association rate constant ( $k_{on}$ ) and dissociation rate constant ( $k_{off}$ ) at controlled temperatures of 19, 25, 31, and 37 °C.

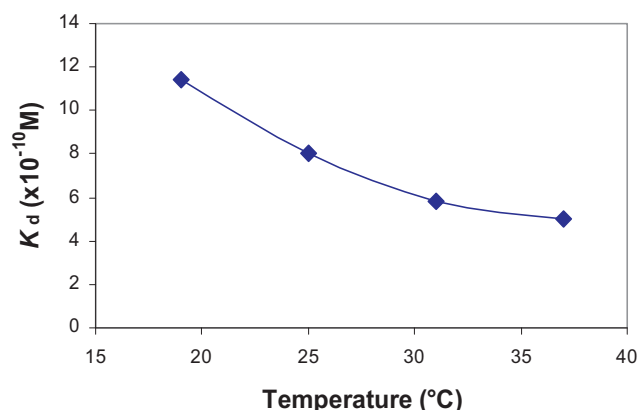


Fig. 10. Equilibrium dissociation constant ( $K_d$ ) at controlled temperatures of 19, 25, 31, and 37 °C.

in solution (typically  $\sim 10^{-10} \text{ M}$ ), which is likely attributable to two reasons. First, the surface-immobilized receptor has restricted conformational flexibility for the analyte to access the entire binding sites [39], and thus may not retain its full solution-based activity [40]. In addition, avidity, in which the binding of analyte molecules with receptor molecules is synergistically stabilized by entropic effects [36], is known to have a noticeable contribution to high-affinity binding systems [41]. In our experiments, the presence of the solid surface may have led to reduced avidity effects because of less efficient diffusion [42] and limited clustering of analyte and receptor molecules [36].

#### 4. Conclusion

This paper presents label-free characterization of temperature-dependent biomolecular affinity binding on solid surfaces using a microcantilever-based device integrating on-chip temperature sensing. The device consists of a Parylene cantilever one side of which is coated with a thin gold film and functionalized with molecules of an affinity receptor to a target analyte. The cantilever is located in a PDMS microfluidic chamber which is integrated with a transparent ITO thin-film resistive temperature sensor on a glass slide. The ITO sensor allows for real-time measurements of the temperature inside the chamber with unobstructed optical access for reflection-based optical detection of the cantilever deflection. The device is situated on a Peltier thermoelectric module, which, in conjunction with the integrated ITO sensor, is used to control the chamber temperature based on a closed-loop PID algorithm. To test the temperature-dependent binding between the target and receptor, the temperature of the chamber is maintained at a

constant setpoint, while the analyte solution is continuously infused through the chamber. The measured cantilever deflection is used to determine the thermodynamic properties associated with the target–receptor binding according to a monovalent binding kinetic model.

We studied the temperature-dependent affinity binding between PDGF, a protein regarded as an ubiquitous mitogen and chemotactic factor in angiogenesis, and an affinity aptamer. We first verified the detection specificity using this device and then systematically characterized the aptamer–PDGF association and dissociation processes with the chamber temperature controlled in the range of 19–37 °C. Quantitative binding properties were obtained, indicating strong temperature dependence of the binding of PDGF to the aptamer. As the temperature increased from 19 to 37 °C, the association rate constant increased from  $1.3 \times 10^7$  to  $2.3 \times 10^7 (\text{M min})^{-1}$ , while dissociation rate constant decreased from 0.015 to  $0.01 \text{ min}^{-1}$ . This corresponds to a decrease of the equilibrium dissociation constant from approximately  $12 \times 10^{-10} \text{ M}$  to  $5 \times 10^{-10} \text{ M}$ . These results provide a starting point for label-free characterization of temperature-dependent biomolecular interactions, and can potentially used for the screening and optimization of inhibiting ligands of PDGF and other target molecules.

#### Acknowledgments

The authors gratefully acknowledge financial support from the National Science Foundation (Award Nos. DBI-0650020 and CBET-0854030) and National Institutes of Health (Award Nos. RR025816-02 and CA147925-01).

#### References

- [1] T. Nguyen, J.P. Hilton, Q. Lin, Emerging applications of aptamers to micro- and nanoscale biosensing, *Microfluidics and Nanofluidics* 6 (2009) 347–362.
- [2] H.-J. Bohm, G. Schneider, *Protein–Ligand Interactions: From Molecular Recognition to Drug Design*, Wiley-VCH, 2003.
- [3] A. Velazquez-Campoy, M.J. Todd, E. Freire, HIV-1 protease inhibitors: enthalpic versus entropic optimization of the binding affinity, *Biochemistry* 39 (2000) 2201–2207.
- [4] T.W. Mayhew, W.T. Windsor, Ligand binding affinity determined by temperature-dependent circular dichroism: cyclin-dependent kinase 2 inhibitors, *Analytical Chemistry* 345 (2005) 187–197.
- [5] G.K. Shoemaker, N. Soya, M.M. Palcic, J.S. Klassen, Temperature-dependent cooperativity in donor–acceptor substrate binding to the human blood group glycosyltransferases, *Glycobiology* 18 (2008) 587–592.
- [6] T. Nguyen, R. Pei, M. Stojanovic, Q. Lin, An aptamer-based microfluidic device for thermally controlled affinity extraction, *Microfluidics and Nanofluidics* 6 (2009) 479–487.
- [7] L. Brunton, J. Lazo, K. Parker, Goodman and Gilman's: *The Pharmacological Basis of Therapeutics*, 11th ed., McGraw-Hill Professional, 2005.
- [8] L.S. Green, D. Jellinek, R. Jenison, A. Ostman, C.-H. Heldin, N. Janjic, Inhibitory DNA ligands to platelet-derived growth factor B-chain, *Biochemistry* 35 (1996) 14413–14424.
- [9] T.K. Dam, R. Roy, D. Page, C.F. Brewer, Negative cooperativity associated with binding of multivalent carbohydrates to lectins. Thermodynamic analysis of the multivalency effect, *Biochemistry* 41 (2002) 1351–1358.
- [10] C.L. Danvic, G. Guiraudie-Capraz, D. Abderrahmani, J.-P. Zanetta, P.N.-L. Meilour, Natural ligands of porcine olfactory binding proteins, *Journal of Chemical Ecology* 35 (2009) 741–751.
- [11] W.-L. Tseng, H.-T. Chang, S.-M. Hsu, R.-J. Chen, S. Lin, Immunoaffinity capillary electrophoresis: determination of binding constant and stoichiometry for antibody–antigen interaction, *Electrophoresis* 23 (2002) 836–846.
- [12] P. Bergese, G. Oliviero, I. Alessandri, L.E. Depero, Thermodynamics of mechanical transduction of surface confined receptor/ligand reactions, *Journal of Colloid and Interface Science* 316 (2007) 1017–1022.
- [13] J. LaBaer, N. Ramachandran, Protein microarrays as tools for functional proteomics, *Current Opinion in Chemical Biology* 9 (2005) 14–19.
- [14] P. Angenendt, J. Glokler, Z. Konthur, H. Lehrach, D.J. Cahill, 3D Protein microarrays: performing multiplex immunoassays on a single chip, *Analytical Chemistry* 75 (2003) 4368–4372.
- [15] P. Cimperman, L. Baranauskienė, S. Jachimovičiūtė, J. Jachno, J. Torresan, V. Michailoviene, J. Matuliene, J. Sereikaite, V. Bumelis, D. Matulis, A quantitative model of thermal stabilization and destabilization of proteins by ligands, *Biophysical Journal* 95 (2008) 3222–3231.

- [16] D.A. Raorane, M.D. Lim, F.F. Chen, C.S. Craik, A. Majumdar, Quantitative and label-free technique for measuring protease activity and inhibition using a microfluidic cantilever array, *Nanoletters* 8 (2008) 2968–2974.
- [17] R. Karlsson, R. Stahlberg, Surface plasmon resonance detection and multispot sensing for direct monitoring of interactions involving low-molecular-weight analytes and for determination of low affinities, *Analytical Biochemistry* 228 (1995) 274–280.
- [18] P.D. Skottrup, M. Nicolaisen, A.F. Justesen, Towards on-site pathogen detection using antibody-based sensors, *Biosensors and Bioelectronics* 24 (2008) 339–348.
- [19] H.-F. Ji, H. Gao, K.R. Buchapudi, X. Yang, X. Xu, M.K. Schulte, Microcantilever biosensors based on conformational change of proteins, *The Analyst* 133 (2008) 434–443.
- [20] A.-R.A. Khaled, K. Vafai, M. Yang, X. Zhang, C.S. Ozkan, Analysis, control and augmentation of microcantilever deflections in bio-sensing systems, *Sensors and Actuators B: Chemical* 94 (2003) 103–115.
- [21] P.W. Snyder, G. Lee, P.E. Marszalek, R.L. Clark, E.J. Toone, A stochastic, cantilever approach to the evaluation of solution phase thermodynamic quantities, *Proceedings of the National Academy of Sciences of the United States of America* 104 (2007) 2579–2584.
- [22] T. Braun, M.K. Ghatkesar, N. Backmann, W. Grange, P. Boulanger, L. Letellier, H.-P. Lang, A. Bietsch, C. Gerber, M. Hegner, Quantitative time-resolved measurement of membrane protein–ligand interactions using microcantilever array sensors, *Nature Nanotechnology* 4 (2009) 179–185.
- [23] M. Yue, J.C. Stachowiak, H. Lin, R. Datar, R. Cote, A. Majumdar, Label-free protein recognition two-dimensional array using nanomechanical sensors, *Nanoletters* 8 (2008) 520–524.
- [24] R. Mukhopadhyay, V.V. Sumbayev, M. Lorentzen, J. Kjems, P.A. Andreasen, F. Besenbacher, Cantilever sensor for nanomechanical detection of specific protein conformations, *Nanoletters* 5 (2005) 2385–2388.
- [25] M.B. Viani, L.I. Pietrasanta, J.B. Thompson, A. Chand, I.C. Gebeshuber, J.H. Kindt, M. Richter, H.G. Hansma, P.K. Hansma, Probing protein–protein interactions in real time, *Nature Structural Biology* 7 (2000) 644–647.
- [26] F. Huber, M. Hegner, C. Gerber, H.-J. Guntherodt, H.P. Lang, Label free analysis of transcription factors using microcantilevers arrays, *Biosensors and Bioelectronics* 21 (2006) 1599–1605.
- [27] S.S. Sinha, R.K. Mitra, S.K. Pal, Temperature-dependent simultaneous ligand binding in human serum albumin, *Journal of Physical Chemistry B* 112 (2008) 4884–4891.
- [28] S.L. Biswal, D. Raorane, A. Chaiken, H. Birecki, A. Majumdar, Nanomechanical detection of DNA melting on microcantilever surfaces, *Analytical Chemistry* 78 (2006) 7104–7109.
- [29] J. Li, E.S. Yeung, Real-time single-molecule kinetics of trypsin proteolysis, *Analytical Chemistry* 80 (2008) 8509–8513.
- [30] Y. Yang, F.-C. Lin, G. Yang, Temperature control device for single molecule measurements using the atomic force microscope, *Review of Scientific Instruments* 77 (2006) 063701.
- [31] B. Wang, J. Ho, J. Fei, R.L. Gonzalez, Q. Lin Jr., A microfluidic approach for investigating the temperature dependence of biomolecular activity with single-molecular resolution, *Lab on a Chip* 11 (2011) 274–281.
- [32] G.A. Richardson, Autonomous thermal control system for highly variable environments, *Journal of Heat Transfer* 131 (2009) 064505 (3 pages).
- [33] B. Yang, Q. Lin, Planar micro check valves based on polymer compliance, *Sensors and Actuators A: Physical* 134 (2007) 186–193.
- [34] R.W. Glaser, Antigen–antibody binding and mass transport by convection and diffusion to a surface: a two-dimensional computer model of binding and dissociation kinetics, *Analytical Biochemistry* 213 (1993) 152–161.
- [35] J. Liu, N.J. Agrawal, A. Calderon, P.S. Ayyaswamy, D.M. Eckmann, R. Radhakrishnan, Multivalent binding of nanocarrier to endothelial cells under shear flow, *Biophysical Journal* 101 (2011) 319–326.
- [36] G.D. Crescenzo, C. Boucher, Y. Durocher, M. Jolicœur, Kinetic characterization by surface plasmon resonance-based biosensors: principle and emerging trends, *Cellular and Molecular Bioengineering* 1 (2008) 204–215.
- [37] G. Prism: [www.graphpad.com/prism/prism.htm](http://www.graphpad.com/prism/prism.htm)
- [38] G. Carta, A. Jungbauer, *Protein Chromatography: Process Development and Scale-Up*, Wiley-VCH, 2010.
- [39] C.A. Savran, S.M. Knudsen, A.D. Ellington, S.R. Manalis, Micromechanical detection of proteins using aptamer-based receptor molecules, *Analytical Chemistry* 76 (2004) 3194–3198.
- [40] R.A. Potyrailo, R.C. Conrad, A.D. Ellington, G.M. Hieftje, Adapting selected nucleic acid ligands (aptamers) to biosensors, *Analytical Chemistry* 70 (1998) 3419–3425.
- [41] G.D. Crescenzo, P.L. Pham, Y. Duracher, M.D. O'Conner-McCourt, Transforming growth factor-beta (TGF- $\beta$ ) binding to the extracellular domain of the type II TGF- $\beta$  receptor: receptor capture on a biosensor surface using a new coiled-coil capture system demonstrates that avidity contributes significantly to high affinity binding, *Journal of Molecular Biology* 328 (2003) 1173–1183.
- [42] M. Gavutis, E. Jacks, P. Lamken, J. Piehler, Determination of the two-dimensional interaction rate constants of a cytokine receptor complex, *Biophysical Journal* 90 (2006) 3345–3355.

## Biographies

**BinWang** received his Ph.D. (2012) in Mechanical Engineering from Columbia University, his B.S. (2003) in Mechanical Engineering from the University of Science and Technology of China (USTC), and M.S. (2006) in Microelectronics and Solid-State Electronics from Shanghai Institute of Microsystem and Information Technology, Chinese Academy of Sciences. His research interests include biomedical applications of microelectromechanical systems (BioMEMS).

**Fengliang Huang** received the M.S. degree in 1994 and Ph.D. degree in 1998, both in Mechanical Engineering, from Northeastern University (China). He was a senior visiting scholar in Columbia University in 2008–2009. He is currently a Professor at Nanjing Normal University. His research interest focuses on advanced sensor technology and intelligent detection systems.

**ThaiHuu Nguyen** received his M.S. (2007) and Ph.D. (2011) in Mechanical Engineering from Columbia University, and his B.S. (2003) in Mechanical Engineering from the University of Virginia. He was a postdoc in the BioMEMS Laboratory at Columbia University in 2011. He is currently a Nuclear Reactor Engineer at Naval Sea Systems Command.

**Yong Xu** received the Ph.D. degree in Electrical Engineering from the California Institute of Technology, Pasadena, in 2002. Then he joined Wayne State University as an Assistant Professor of Electrical Engineering and currently he holds an Associate Professor at Wayne State University. His research interests are in MEMS, biomedical electronics, and nanotechnology.

**QiaoLin** received the Ph.D. degree in Mechanical Engineering from the California Institute of Technology, Pasadena, in 1998, with thesis research in robotics. He conducted postdoctoral research in microelectromechanical systems (MEMS) at the Caltech Micromachining Laboratory from 1998 to 2000 and was an Assistant Professor of mechanical engineering at Carnegie Mellon University, Pittsburgh, PA, from 2000 to 2005. He has been an Associate Professor of mechanical engineering at Columbia University, New York, NY, since 2005. His research interests are in designing and creating integrated micro/nanosystems, particularly MEMS and microfluidic systems, for biomedical applications.